

Direct and Rb-promoted $\text{SiO}_x/\beta\text{-SiC}(100)$ interface formation

M. Riehl-Chudoba* and P. Soukiassian

*Commissariat à l'Energie Atomique, DSM-DRECAM-SRSIM, Bâtiment 462, Centre d'Etudes de Saclay,
91191 Gif sur Yvette Cedex, France
and Département de Physique, Université de Paris-Sud, 91405 Orsay Cedex, France*

C. Jaussaud

LETI (CEA-Technologies Avancées), DMEL, CEN/G, 85 X, 38041 Grenoble Cedex, France

S. Dupont†

*Commissariat à l'Energie Atomique, DSM-DRECAM-SRSIM, Bâtiment 462, Centre d'Etudes de Saclay,
91191 Gif sur Yvette Cedex, France*

(Received 7 March 1994; revised manuscript received 30 November 1994)

We investigate the formation of $\text{SiO}_x/\beta\text{-SiC}(100)$ interfaces by direct and Rb-promoted oxidation by means of photoemission spectroscopy using the $\text{Al } K\alpha$ (1486.6-eV) and $\text{Zr } M_\zeta$ (151.4-eV) x-ray lines at Si 2p, C 1s, O 1s, and Rb 3p core levels. Clean and stoichiometric $\beta\text{-SiC}(100)$ surfaces have been obtained applying thermal annealing treatments only. Room-temperature Rb deposition on the clean $\beta\text{-SiC}(100)$ surface induces a large decrease of the work function, reaching a minimum with $\Delta\Phi = -3.3$ eV. This work-function change corresponds to the Rb saturation coverage of one physical monolayer (1 Rb ML). Room-temperature exposure of the clean $\beta\text{-SiC}(100)$ surface to molecular oxygen results in only little oxygen uptake and small amounts of silicon oxide, showing no evidence of bonding between carbon and oxygen atoms on the surface. When the $\beta\text{-SiC}(100)$ surface is modified by a Rb monolayer, the oxygen uptake is dramatically enhanced by four orders of magnitude, leading to a large increase of the oxidation rate and forming high silicon oxidation states. The oxygen atoms appear to be more tightly bound to Si than to Rb atoms while, as in the case of direct oxidation, there is apparently no sign of carbon-oxygen bonding present on the surface, which can be explained by formation of CO or CO_2 species desorbing into the vacuum. Upon thermal annealing at temperatures up to 700°C, the oxide layer thickness is increased with a significant improvement of the stoichiometry, leading to the formation of a nonabrupt carbon-free $\text{SiO}_2/\beta\text{-SiC}(100)$ interface including lower oxidation states at the interface. The Rb overlayer is removed from the surface by thermal desorption below 780°C.

I. INTRODUCTION

Silicon carbide is a promising IV-IV compound semiconductor, in particular with respect to potential applications in electronics. In fact, this "refractory" semiconducting material, having a wide band gap and a high thermal stability, could be very useful for operation at rather elevated temperatures ($\geq 600^\circ\text{C}$), especially when compared to silicon ($< 150^\circ\text{C}$), and makes it especially suitable for high-power and high-temperature electronic devices; see Ref. 1. Furthermore, depending on whether its structural phase is cubic (β) or hexagonal (α), silicon carbide also appears as a promising alternative to III-V compound semiconductors in fast electronic devices. However, in contrast to many other elemental or compound semiconductors, silicon carbide has received much less attention in surface and interface science. This situation is mainly due to the difficulties encountered in the growth of high-quality single crystals. Former investigations have been mainly focused on surface preparation and on the surface structure, including in the latter case some very recent theoretical investigations.²⁻²⁰ Adsorption studies were primarily oriented towards metal adsorbates with a special emphasis on metal/SiC interface formation.¹⁹⁻²⁴ However, only few studies were so far

oriented to another very important issue, i.e., the silicon carbide surface passivation, especially by surface oxidation,^{25,26} which is a very important step in the production of electronic devices. While it is rather easy to grow oxide insulator films on silicon surfaces, the oxidation process could in some cases turn out to be very different when silicon is forming an alloy.²⁷ In fact, when compared to silicon, silicon carbide is a semiconductor on which it is rather difficult to grow native oxides.

In order to grow oxide layers on SiC with reasonably high formation rates, a metal catalyst providing a stronger interaction between oxygen molecules and the surface could be used. Many metals, including aluminum, noble, transition, and rare-earth metals, have been shown to promote the oxidation of silicon and some other semiconductors.^{27,28} However, in all these cases, the mechanisms of promotion generally include surface disruption associated with diffusion into the bulk and silicide formation.^{27,28} This leads to oxides intermixed with the metal catalyst, which might affect the overall dielectric properties and result in some detrimental effects for electronic device applications. In the recent years, alkali-metal atoms have been shown to act as very efficient promoters of semiconductor or metal oxidation.²⁹⁻³⁸ The presence of an alkali-metal layer on the

surfaces of elemental group-IV materials such as silicon or graphite, III-V compound semiconductors, and metals like aluminum has been found to enhance the oxidation rate by 4 to 13 orders of magnitude.^{29–42} Furthermore, unlike other metals, the alkali catalyst could be removed from the surface by thermal annealings at moderate temperatures in the case of silicon and aluminum surfaces only.^{29–33,36–38} For all these surfaces, the micromechanisms of alkali-metal-promoted oxidation present some common features including the weakening of the surface atom back bonds, the drastic increase of the oxygen molecule sticking coefficient, and its efficient dissociation by charge transfer into the antibonding molecular orbitals.^{29,31,33,35,37,39} Furthermore, the migration of oxygen atoms underneath the surface is facilitated, which favors the bonding with the substrate atoms.^{31,33} However, some striking differences in the various steps of catalysis were found, depending on substrate nature. While oxygen atoms remain weakly bonded to the alkali catalyst on semiconductor surfaces with no alkali oxide formation, clear evidence of Na or K oxide growth was shown in the case of alkali-metal-promoted oxidation of aluminum.³⁸ Furthermore, unlike elementary semiconductors, surface defects seem to play a central role for III-V compound semiconductors, which, in contrast to Si, generally form, at room temperature, rather chemically reactive interfaces with alkali-metal atoms.⁴⁰ Finally, one should also notice that, despite very close electronic and structural properties with silicon surface,⁴¹ the oxidation of germanium is, in contrast, inhibited by alkali-metal atoms at room temperature.⁴² In these views, it is of particular interest to study the effect of an alkali-metal overlayer on the oxidation of a compound IV-IV semiconductor such as silicon carbide, which is known to be hard to oxidize when compared to silicon.

In this paper, we present a comprehensive investigation on the direct and Rb-promoted oxidation of a cubic $\beta\text{-SiC}(100)$ surface by means of x-ray photoemission spectroscopy. After the description of surface preparation and the deposition of Rb atoms, we demonstrate that the presence of a Rb monolayer enhances the oxygen uptake by four orders of magnitude at room temperature, favoring the formation of high silicon oxidation states. We also investigate the effect of subsequent annealing, leading to a SiO_x layer with improved stoichiometry containing no carbon related species, likely due to the formation of CO or CO_2 molecules desorbing into the vacuum. The Rb atoms could be removed from the surface by desorption after thermal annealing at moderate temperatures. In this way, a carbon-free $\text{SiO}_2/\beta\text{-SiC}(100)$ interface can be achieved at much lower temperature than by direct oxidation. Our results are also discussed in the context of earlier works performed for silicon and III-V compound semiconductors, for which the role of alkali-metal atoms in the various steps of promoted oxidation and other enhanced-surface reactions is better understood.

II. EXPERIMENTAL DETAILS

The core-level x-ray photoemission spectroscopy (XPS) experiments were performed in an ultrahigh vacuum ex-

perimental system using the Al $K\alpha$ (1486.6-eV) and Zr M_ζ (151.4-eV) lines at Si $2p$, C $1s$, O $1s$, and Rb $3p$ core levels. The photoelectron kinetic energy was measured using a hemispherical electrostatic analyzer (CLAM 2 by VG Microtech) having a mean radius of 100 mm. The x-ray sources were extremely carefully outgassed. In these conditions, the data were acquired at a working pressure better than 6×10^{-11} Torr. Cubic $\beta\text{-SiC}(100)$ single crystal samples were prepared on a Si(100) wafer substrate by chemical vapor deposition (CVD) leading to the formation of a SiC thin film having a thickness of about 1 μm .⁴³ The structure was characterized by conventional x-ray diffraction showing the formation of single crystal silicon carbide. The native oxides, carbon, and other impurities were removed from the surface by sequences of thermal annealings up to 1100 °C. This treatment yields a stoichiometric SiC(100) surface free from contaminant as controlled by XPS. Details about this surface cleaning process are given in Sec. III A. Pure Rb was deposited onto the SiC(100) surface with a SAES chromate dispenser. In order to avoid any codeposition of impurities which could dramatically affect the Rb mode of growth, as we have shown recently for other alkali-metal atoms on silicon surfaces, the Rb source was extremely well outgassed in order to keep the pressure increase during rubidium deposition always below $\Delta P \leq 1 \times 10^{-11}$ Torr.⁴⁴ We have also measured the work-function changes upon Rb deposition using the secondary electron cutoff observed in the photoemission spectra as already described previously.⁴⁵ Surface exposures to a well-defined quantity of oxygen molecules (research grade) were performed through a tube leading directly to the sample.³⁷ All other experimental details can be found elsewhere.^{37,44}

III. RESULTS

A. $\beta\text{-SiC}(100)$ surface preparation by thermal annealings

The first problem to address is obtaining a clean and stoichiometric silicon carbide surface, which is not as easy to achieve as for other semiconductor surfaces. The Si $2p$, C $1s$, and O $1s$ core-level spectra of the $\beta\text{-SiC}(100)$ surface are presented in Fig. 1 for the “as received” sample and after several annealings at temperatures ranging from 360 to 1100 °C. The “as received” sample exhibits components with large chemical shifts for both Si $2p$ and C $1s$ core-level spectra (see bottom curves). For Si $2p$ the chemically shifted component indicates the presence of native silicon oxide on the surface. The C $1s$ core level has a 2-eV shifted component (C_x) located at the high binding energy side. This feature is due to the presence of carbon atoms on the surface (probably as clusters or as graphite) and also likely to hydrocarbon molecules both resulting from the CVD process.⁴³ The intense O $1s$ core level results from the presence of silicon oxide (SiO_x), as observed at the Si $2p$ core level. When the “as received” $\beta\text{-SiC}(100)$ surface is subjected to annealings, one can see at both Si $2p$ and O $1s$ core levels that increasing temperatures induce the gradual decomposition and removal of the oxide, which is completely eliminated at 1100 °C.

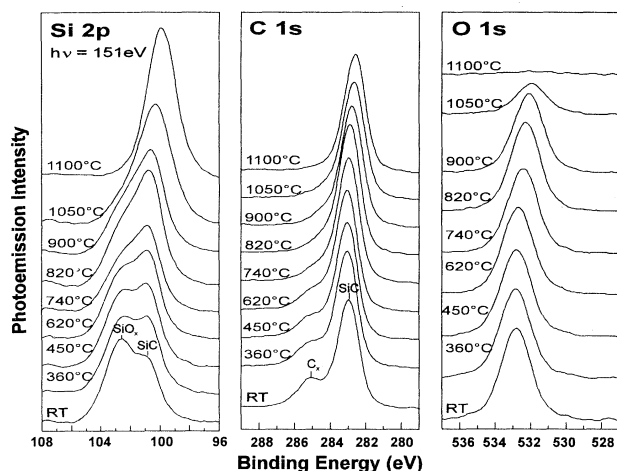


FIG. 1. Si 2*p*, C 1*s*, and O 1*s* core levels for the “as received” SiC(100) surface (bottom spectra) and after annealings ranging from 360 to 1100°C. The photon energies were 151.4 eV (Si 2*p*) and 1486.6 eV (C 1*s* and O 1*s*).

During the same annealing sequence, the C 1*s* shows a gradual decrease of its C_x component, indicating the desorption of the carbon related contaminants or graphite clusters. After annealing at 1100°C, the β -SiC(100) surface is free of oxygen and carbon contaminants, while the Si 2*p* and C 1*s* line positions correspond respectively to the binding energies of Si fourfold bonded to C and vice versa, which indicates the presence of a clean and stoichiometric silicon carbide surface.

In order to have a better estimation of the surface stoichiometry, we have plotted the C 1*s* and Si 2*p* intensity ratio, weighted by the relative sensitivity factors determined by Wagner *et al.*,⁴⁶ versus the annealing temperatures (Fig. 2, bottom), and compared it to the corresponding O 1*s* integrated intensity (Fig. 2, top). As can be seen in the top panel of Fig. 2, the oxygen loss becomes significant only above 800°C as a result of SiO_x desorption. The bottom panel of Fig. 2 shows that, while the “as received” substrate is carbon rich, the C/Si ratio gradually decreases with increasing annealing temperature, reaching finally 1 at 1100°C. This shows that a clean and stoichiometric β -SiC(100) surface can be obtained only by thermal annealings, and that surface ion sputtering, which might leave Ar atoms embedded in the surface or create defects, is not necessary. Figure 3 compares the large scan (from 80 to 320 eV) spectra for the β -SiC(100) surface (dashed line) after annealing at a temperature of 1100°C and for a clean Si(100)2×1 surface (solid line), showing the Si 2*p* and C 1*s* core-level lines. One can observe the characteristic silicon and silicon carbide plasmon loss features, which are located at 17 eV (Si) and 22 eV (SiC), respectively, apart from the core-level lines, which is in excellent agreement with previous works.^{8,47}

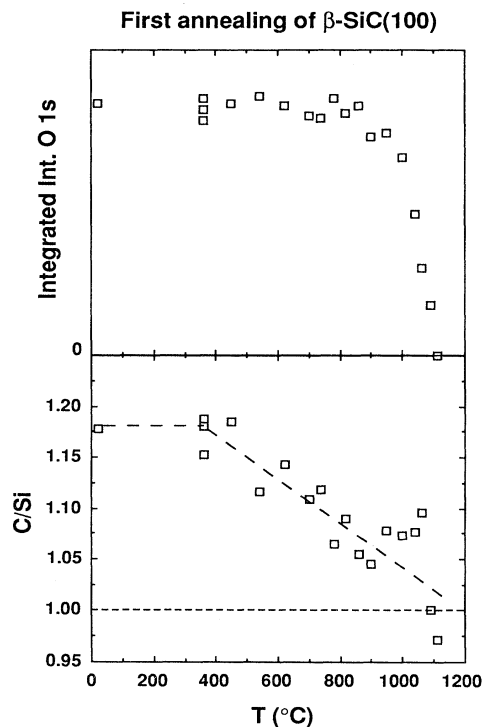


FIG. 2. Top: O 1*s* integrated intensity vs annealing temperature (extracted from Fig. 1). Bottom: C 1*s*/Si 2*p* integrated intensity ratio weighted by the relative sensitivity factors determined by Wagner *et al.* (Ref. 45) vs annealing temperature (extracted from Fig. 1). A dashed line has been drawn as a visual guide.

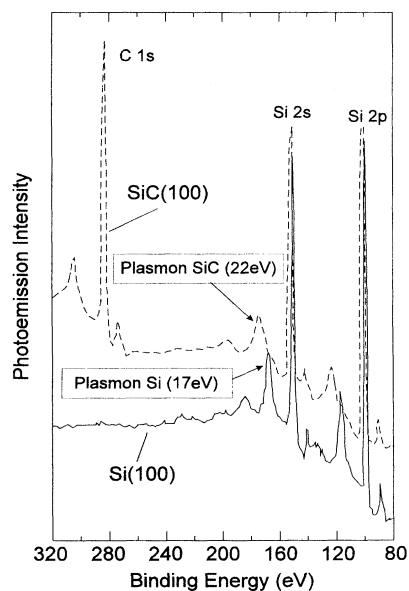


FIG. 3. Wide scan XPS spectra for a clean β -SiC(100) surface (dashed line) and a clean Si(100) surface (solid line) showing the Si 2*p* and C 1*s* core-level lines and the characteristic plasmon loss features (SiC: 22 eV; Si: 17 eV).

B. Rb mode of growth and work-function changes for Rb/SiC(100)

The Rb mode of growth on the SiC(100) surface is illustrated by the Rb 3*p* core-level integrated intensity and surface work-function changes as a function of the alkali-metal evaporation time, which are, respectively, shown in the top and bottom panels of Fig. 4. Upon increasing Rb evaporation time, the Rb 3*p* core-level integrated intensity shows a linear behavior up to an evaporation time of 140 s, after which saturation is reached.

This mode of growth is very similar to what we have observed for other alkali-metal atoms on nonreactive surfaces, such as SiC(100)2×1, reaching a saturation coverage at room temperature. This saturation coverage corresponds to one monolayer, meaning one “physical” alkali-metal layer, as explained previously for other alkali-metal-covered semiconductor surfaces.⁴⁴ It indicates that, at room temperature, the Rb sticking coefficient becomes negligible on SiC(100) at the completion of a monolayer. Further information about the Rb uptake can be found in bottom panel of Fig. 4, which displays the corresponding work-function change $\Delta\Phi$. We can see that $\Delta\Phi$ decreases linearly with the Rb coverage reaching the lowest work-function value with $\Delta\Phi = -3.3$ eV at the Rb saturation coverage. The work function does not change any more beyond the Rb saturation coverage. Again, this behavior is very similar to what has been observed for alkali-metal-covered silicon surfaces, where work-function minima have been found at values ranging from -3 , -3.2 , and -3.4 eV, respec-

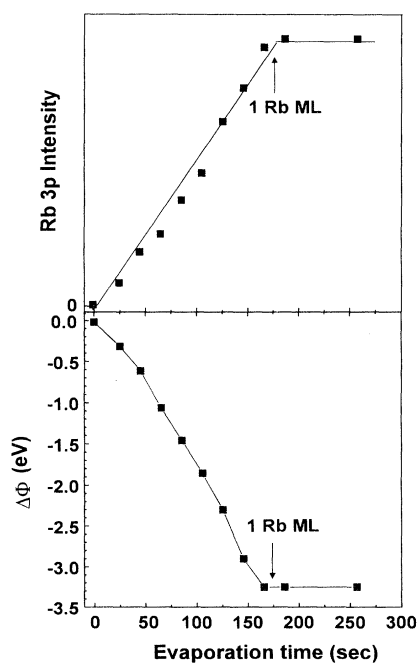


FIG. 4. Top: Rb 3*p* integrated intensity vs Rb deposition time on $\beta\text{-SiC}(100)$. Bottom: Work-function change $\Delta\Phi$ vs Rb deposition time for Rb/ $\beta\text{-SiC}(100)$. An arrow indicates the completion of the saturation coverage corresponding to one Rb monolayer.

tively, for Na, K, and Cs on the Si(100)2×1.^{48–50} This work-function change, which is a well-known feature of alkali-metal adsorption on surfaces, is understood in terms of the formation of a polarized bonding between the alkali-metal atom and the substrate surface.⁵¹ The results suggest that the bonding of Rb on SiC appears to be, in analogy to the Si substrate, nonreactive in nature. However, in order to draw a definitive conclusion about this important issue, high-resolution photoemission experiments using synchrotron radiation are necessary.

C. Direct and Rb-promoted oxidation at room temperature

We now investigate the effect of a Rb monolayer on the room-temperature oxygen uptake and on the SiC(100) surface oxidation. For comparison, we first study the direct SiC oxidation by molecular oxygen exposures of the bare SiC(100) surface. Figure 5 displays the Si 2*p* and O 1*s* core-level spectra taken after exposures ranging from 10^{+15} to 10^{+19} oxygen molecules. Upon such a sequence, the O 1*s* core-level intensity gradually increases, indicating the progressive sticking of oxygen molecules on the surface. However, a significant O 1*s* intensity is achieved only at exposures higher than 10^{+16} molecules of O_2 . The silicon oxide formation can be followed at the Si 2*p* core level which exhibits a slight core-level shift on the high binding energy side only at oxygen exposures larger than 10^{+18} molecules. This shows that, while molecular oxygen is adsorbed on the $\beta\text{-SiC}(100)$ surface, the resulting silicon oxide formation remains limited to

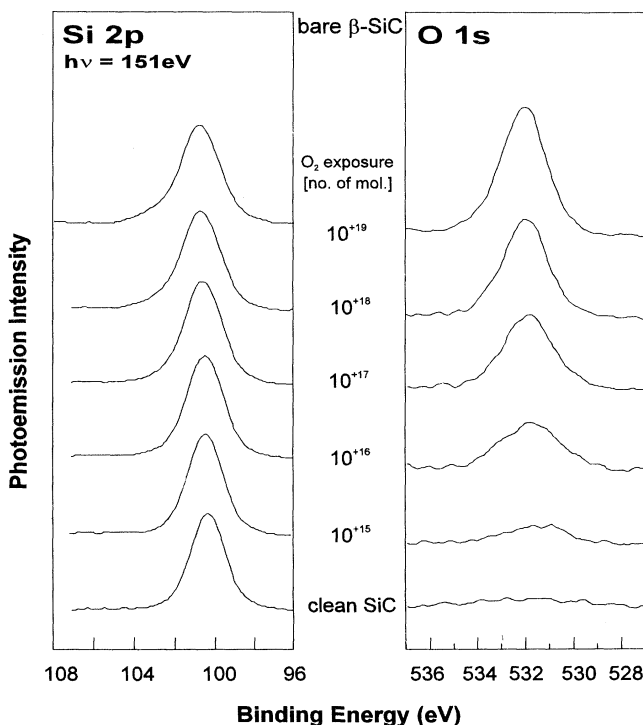


FIG. 5. Si 2*p* and O 1*s* core-level spectra taken after oxygen exposures of a bare $\beta\text{-SiC}(100)$ surface ranging from 10^{+15} to 10^{+19} molecules O_2 . The photon energies were 151.4 eV (Si 2*p*) and 1486.6 eV (O 1*s*).

small amounts only. This situation differs significantly from the case of a Si substrate, where similar exposures result in more important silicon oxide growth on the surface.⁵² Unfortunately, the experimental resolution which could be achieved with an x-ray source (≈ 1.0 eV) does not allow a straightforward identification of the single Si oxidation states, as performed when using synchrotron radiation.^{33,52} However, from the shoulder at the high binding energy side of the Si $2p$ core level, one can reliably estimate the presence of predominantly lower oxidation states such as Si^{1+} and Si^{2+} . In contrast, the C $1s$ core-level line does not exhibit any apparent change when following the same oxygen exposure sequence. This behavior indicates the lack of C—O bond formation present on the surface.

After the direct SiC oxidation, we now turn to the Rb-promoted oxidation at room temperature. Figure 6 displays the Si $2p$ and O $1s$ core-level spectra for a β -SiC(100) surface modified by a Rb monolayer, for the same molecular oxygen exposure sequence as in the direct oxidation presented above (Fig. 5). We first remark that the presence of the Rb overlayer significantly increases the oxygen sticking coefficient, especially at the very beginning of the chemisorption process, showing a much larger intensity of the O $1s$ core level already at the lowest O_2 exposure of 10^{+15} molecules. Furthermore, the O $1s$ core level clearly exhibits two components *A* and *B*, in contrast to the case of direct oxidation, which has also been found recently for the K and Cs promoted

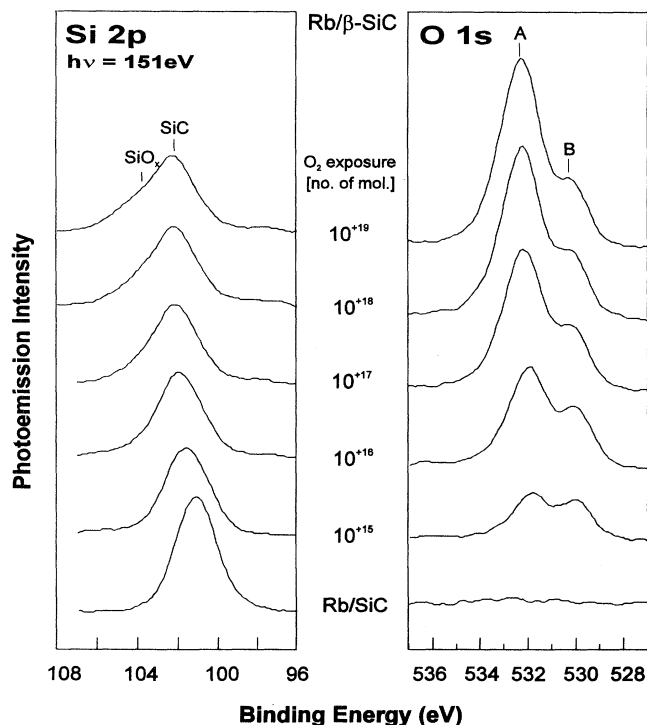


FIG. 6. Si $2p$ and O $1s$ core-level spectra taken after oxygen exposures of a Rb-saturated β -SiC(100) surface ($\Theta_{\text{Rb}} = 1$ ML) ranging from 10^{+15} to 10^{+19} molecules O_2 . The photon energies were 151.4 eV (Si $2p$) and 1486.6 eV (O $1s$).

Si(100) 2×1 oxidation.^{34,37} The peak *A* corresponds to oxygen atoms bonded to the substrate, i.e., predominantly to silicon, which can be deduced from its energetic position and its relation to the intensity of the Si $2p$ chemically shifted component. The O $1s$ component *B* located at lower binding energy can be related to oxygen bonded to the Rb adsorbate, since its intensity scales with the amount of alkali-metal atoms present on the surface. The growth of silicon oxide products can be observed at the Si $2p$ core level (Fig. 6) showing an intense chemically shifted component, which indicates the formation of much larger SiO_x amounts on Rb/ β -SiC(100) as compared to the bare surface. In contrast, the C $1s$ spectra do not exhibit any change upon Rb deposition and/or oxygen exposure, which again is a sign for the absence of any apparent carbon-oxide species on the surface.

In order to follow the oxygen uptake on the clean and Rb-promoted β -SiC(100) surface, we have plotted in Fig. 7 the integrated intensities for the total O $1s$ core level and also for its *A* and *B* components extracted from Figs. 5 and 6. Basically, the total oxygen uptake increases almost linearly with the logarithm of oxygen molecules for both direct and Rb-promoted β -SiC(100) surface oxidation. Furthermore, while the integrated intensity of O $1s$ component *A* (O atoms bonded to Si) also follows the same linear trend, the O $1s$ component *B* (O atoms bonded to Rb) is already saturated at the smallest oxygen exposure (10^{+15} molecules) and remains constant also after higher exposures. This behavior appears to be very similar to the case of alkali-metal-promoted oxidation of the Si(100) 2×1 surface.³⁷ In addition, by comparing the O $1s$ core level total integrated intensities for β -SiC(100) and Rb/ β -SiC(100) surfaces at O_2 exposures of 10^{+15} and 10^{+19} molecules, one can remark that the presence of Rb increases the oxygen uptake by four orders of magnitude. The magnitude of the promotion effect that is observed is comparable to the case of silicon, but significantly smaller when compared to III-V compound semiconductors, where the oxidation rate could be enhanced by factors

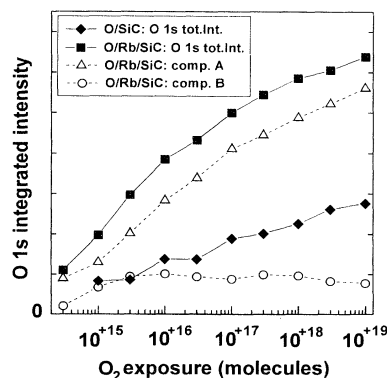


FIG. 7. O $1s$ total integrated intensity for O_2/β -SiC(100) and $\text{O}_2/\text{Rb}/\beta$ -SiC(100) surfaces vs the logarithm of the oxygen exposures extracted from Figs. 5 and 6 ($\Theta_{\text{Rb}} = 1$ ML). The integrated intensities of O $1s$ *A* (related to O—Si bonds) and *B* (related to O—Rb bonds) components have also been plotted for the $\text{O}_2/\text{Rb}/\beta$ -SiC(100) surface using the same scale.

ranging from 10^{+6} to 10^{+13} .^{40,53} Also, it is interesting to notice that, upon Rb-promoted oxidation, silicon carbide behaves very differently from other compound semiconductors such as III-V. In the latter case, such a linear dependence of oxygen uptake versus the logarithm of oxygen exposures is not observed, with a trend to saturation at the higher exposures,^{35,53} which is probably due to a more complex interface formation.⁴⁰

D. Effect of thermal annealings on the Rb-promoted oxidation

After the description of our results for the room temperature Rb-promoted oxidation, we now turn to the effect of thermal annealings. Figure 8(a) shows the Si 2*p* and O 1*s* core-level spectra for the Rb-saturated $\beta\text{-SiC}(100)$ surface after exposure to 10^{+19} oxygen molecules and subjected to rapid thermal annealings (RTA) at various temperatures ranging from 330 to 950 °C. Upon increasing temperatures, the Si 2*p* chemical shifted component related to silicon oxides exhibits an increase of intensity and a shift to higher binding energies. This behavior indicates the formation of a larger silicon oxide layer having an improved stoichiometry. After annealing at 440 °C, a significant intensity of the Si 2*p* oxide related component is visible at a binding energy at 103.9 eV indicating the formation of stoichiometric SiO_2 , while lower Si oxidation states (Si^+ , Si^{2+} , and Si^{3+}) are still present as in the case of direct and alkali-metal-promoted silicon oxidation.^{31,33} The C 1*s* and Si 2*p* core-level spectra taken in a bulk sensitive mode with the Al *K* α line indicate that the $\text{O}_2/\text{Rb}/\text{SiC}(100)$ surface exhibits a change of the Fermi level position due to band bending giving rise to a rigid shift at the core-level lines by about 0.4 eV to higher binding energies. Therefore, it can be concluded that the energy position in the SiC state of the Si 2*p* spectra is located at a slightly lower binding energy with respect to the Si 2*p* maximum [see marker in Fig. 8(a)]. This could be explained by the contribution of the low Si oxidation states (Si^+ , Si^{2+}) having a slightly higher binding energy, which are likely present at the surface and/or interface. At annealing temperatures above 780 °C, the amount of silicon oxides starts to decrease, becoming negligible at 950 °C. This results from the desorption of volatile Si-O species initiated at temperatures around 800 °C.³⁶ Additional information about the effect of thermal annealings can be obtained by looking at the O 1*s* core-level spectra for the same sequence [Fig. 8(a), right panel]. The O 1*s* component B (related to O—Rb bonds) is decreasing with increasing temperatures and becomes negligible after annealing at about 700 °C, with component A (related to O—Si bonds) remaining the only spectral feature. As we will see later, this behavior results from the gradual thermal desorption of the Rb catalyst. The intensity of the O 1*s* A component is dramatically reduced at 950 °C in agreement with silicon oxide decomposition and Si-O desorption also evidenced in the Si 2*p* spectra.

The corresponding spectra of the C 1*s* and Rb 3*p* core levels for the same sequence of thermal annealings are presented in Fig. 8(b). As already observed above for both direct and Rb-promoted oxidation, the C 1*s* core level remains also basically unchanged upon the thermal

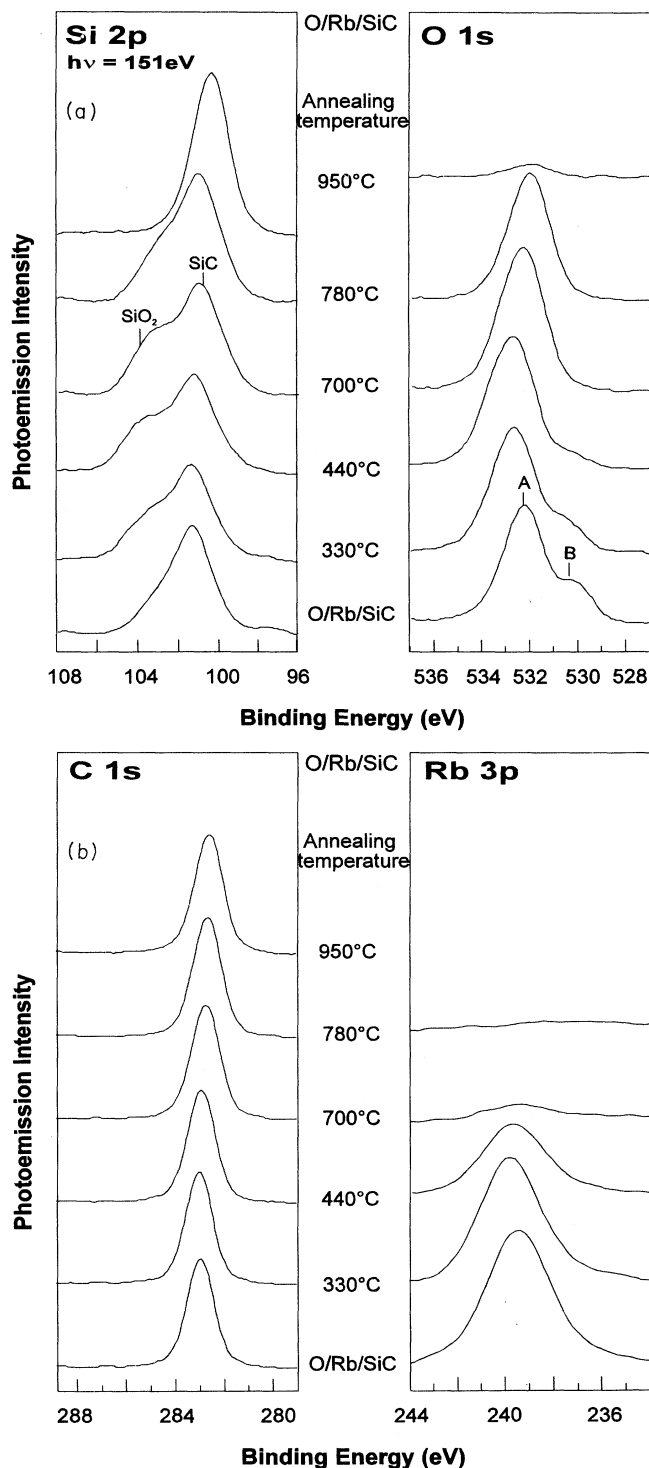


FIG. 8. (a) Si 2*p* and O 1*s* core-level spectra for the $\text{O}_2/\text{Rb}/\beta\text{-SiC}(100)$ surface taken after various thermal annealings at temperatures ranging from 330 to 950 °C ($\Theta_{\text{Rb}}=1$ ML; O_2 exposure = 10^{+19} molecules). The photon energies were 151.4 eV (Si 2*p*) and 1486.6 eV (O 1*s*). (b) C 1*s* and Rb 3*p* core-level spectra for the $\text{O}_2/\text{Rb}/\beta\text{-SiC}(100)$ surface taken after various thermal annealings at temperatures ranging from 330 to 950 °C ($\Theta_{\text{Rb}}=1$ ML; O_2 exposure = 10^{+19} molecules). The photon energy was 1486.6 eV.

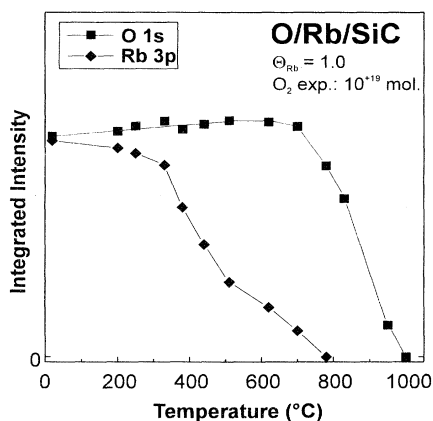


FIG. 9. O 1s and Rb 3p integrated intensities [extracted from Figs. 8(a) and 8(b)] vs the annealing temperature for the $O_2/Rb/\beta\text{-SiC}(100)$ surface ($\Theta_{Rb}=1$ ML; O_2 exposure = 10^{+19} molecules).

annealings. In contrast, the Rb 3p core-level intensity decreases gradually with increasing temperatures to disappear completely between 700 and 780°C. This indicates that the Rb overlayer has been removed from the surface by thermal desorption as previously reported for alkali-metal-promoted silicon surfaces.^{29–31} However, one should notice that the Rb removal observed here for $\beta\text{-SiC}(100)$ occurs at slightly higher temperatures when compared to alkali-metal atoms on Si surfaces, where the temperatures of the complete alkali-metal desorption range from 550°C for Na, 600°C for K, and 650°C for Rb and Cs.^{29–31,33} This suggests that Rb atoms might be significantly more tightly bound to the surface of $\beta\text{-SiC}(100)$ than to the Si(100) one. Anyway, this important point requires a more specific and detailed investigation of the Rb/ $\beta\text{-SiC}(100)$ interface formation.

In order to better compare the effects of annealings on the behavior of Rb and O adsorbates on the $\beta\text{-SiC}(100)$ surface, we have plotted in Fig. 9 the O 1s and Rb 3p total integrated intensities [extracted from Figs. 8(a) and 8(b)] versus the annealing temperature. Interestingly, we can see that the amount of oxygen present on the surface remains basically constant from room temperature up to 700°C, with an onset of decrease around 780°C and total oxygen removal at 1000°C. This indicates that, upon increasing temperature, oxygen is transferred from Rb influenced adsorption sites to Si atoms in the substrate, thereby contributing to the growth of additional oxides and to the improvement in the silicon oxide stoichiometry as observed in the Si 2p spectra. The Rb 3p integrated intensity shows a different behavior upon increasing temperatures with three different regimes including (i) a slight decrease from room temperature to 350°C, (ii) a change of slope with very rapid decrease between 350 and 600°C and, (iii) after another slight change of slope, a linear decrease up to 780°C corresponding to Rb removal from the surface by desorption. One should note that the temperature of 500°C corresponds approximately to the threshold of silicon dioxide formation. A

linear decrease of the alkali catalyst versus annealing temperature has also been observed for Si(100)2×1-promoted oxidation after SiO_2 formation,^{29,31} which provides a consistent behavior for the thermal desorption of alkali-metal atoms from a silicon oxide layer on both substrates.

IV. DISCUSSION

The results presented above demonstrate that rubidium acts as an efficient promoter of $\beta\text{-SiC}(100)$ surface oxidation. While direct oxygen exposures result only in the formation of very small amounts of SiO_x (Fig. 5), the presence of a Rb monolayer enhances the oxygen uptake by four orders of magnitude as can be seen in Fig. 7. Furthermore, the corresponding $\beta\text{-SiC}(100)$ surface oxidation rate is also significantly improved. In fact, for both room-temperature oxidation and upon thermal annealing, the Rb-modified $\beta\text{-SiC}(100)$ surface exhibits larger amounts of silicon oxides. This can be evidenced by looking at the Si 2p core level presented in Fig. 10, which allows an easy comparison between direct and Rb-promoted oxidation at room temperature and after an annealing at 440°C. The promotion effect appears to be more pronounced at elevated temperatures. It results from the transfer of oxygen atoms initially bonded at Rb-influenced sites at room temperature to Si substrate atoms by Rb—O bond breaking upon thermal annealings. This interpretation is evidenced from the disappearance of the O 1s B component (related to O species bonded to Rb) at elevated temperatures [Figs. 8(a) and 10], while the

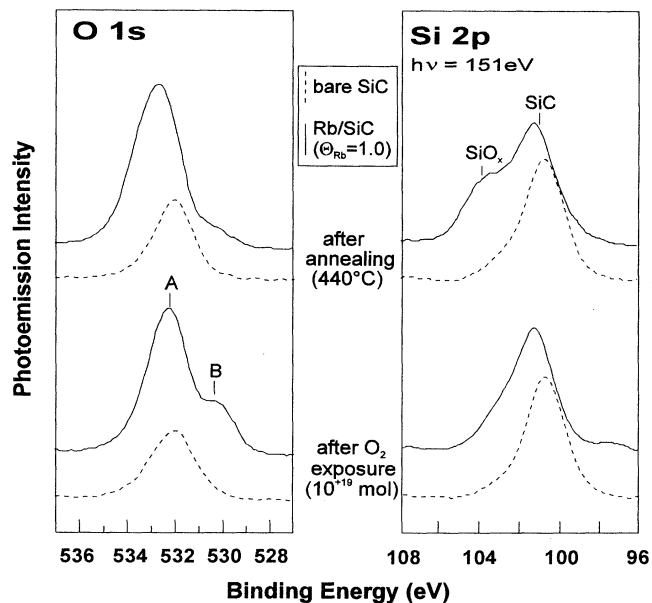


FIG. 10. O 1s and Si 2p core-level spectra comparing the oxygen uptake and oxidation of bare $\beta\text{-SiC}(100)$ (dashed lines) and Rb-saturated $\beta\text{-SiC}(100)$ ($\Theta_{Rb}=1$ ML; solid lines) after room-temperature oxygen exposure (10^{+19} molecules) and after subsequent annealing at 440°C. The photon energies were 151.4 eV (Si 2p) and 1486.6 eV (O 1s).

O 1s total integrated intensity remains constant up to 700°C (Fig. 9). One should note that at 700°C, the O 1s component *A* (related to O atoms bonded to Si) is the only dominant feature, which further supports the picture that oxygen atoms are transferred from rubidium to silicon atoms. As can be deduced from the Si 2*p* core-level spectra in Fig. 8(a), the thermally activated migration of oxygen atoms towards the bulk contributes to the additional Si oxide growth.^{31,33}

Besides the O—Si bond establishment leading to silicon oxide formation, the Rb-promoted oxidation does not show any evidence of O—C bonds present on the surface, which has already been observed also for the direct oxidation of SiC.^{10,25–27} In order to illustrate this point and to trace the existence of a possible core-level shift at C 1s, we compare in Fig. 11 the Si 2*p* and C 1s core-level spectra both recorded in a bulk sensitive mode at a photon energy of 1486.6 eV (Al *K*α), after Rb-promoted oxidation and subsequent thermal annealing at 700°C. In order to visualize the presence of a chemically shifted component, the data have been fitted with a single peak Gaussian (solid line), having a fixed width as extracted from the clean substrate spectrum (bottom curves). By comparing with the latter spectrum, one can see the lack of any change for the C 1s core level in contrast to Si 2*p* showing oxide formation even in the bulk sensitive mode. This situation significantly differs from the case of alkali-metal-promoted oxidation of other compound semiconductors, such as GaAs(110), InP(110), or GaSb(110), where both cation and anion oxides were formed.^{40,53,54} However, alkali-metal atoms were shown to promote also the oxidation of carbon as graphite.^{55,56} Therefore, it is very likely that such an oxidation also takes place here with the formation of CO or CO₂ species, which are

desorbed already at room temperature. In fact, an intermediate compound such as oxygen atoms bridge-bonded to both C and Si appears not to be stable at the surface as evidenced from the lack of any shifted component at C 1s [Figs. 8(b) and 11], which should clearly be visible in the presence of C—O bonding. Anyway, one can easily imagine that the O—Si bond formation subsequently results in C—Si bond breaking. In principle, this process should leave carbon atoms on the surface (as clusters and/or graphite). Apparently, this is not the case, since we do not observe any corresponding spectral feature at the C 1s core level [Figs. 8(b) and 11] as on the “as received” $\beta\text{-SiC}(100)$ surface (Fig. 1). Since, as mentioned above, alkali-metal atoms do promote also the oxidation of graphite surfaces,^{55,56} the only remaining possibility to explain this behavior is that the carbon atoms released during the silicon-oxygen bond establishment are also oxidized. The resulting oxidation products are likely to include CO or CO₂ molecules, which leave the surface by thermal desorption. A similar scenario has already been proposed in the case of the direct oxidation of the hexagonal $\alpha\text{-SiC}$ phase at 1100°C.¹⁰ During the direct and Rb-promoted oxidation process, there is a dynamic equilibrium between Si—C bond breaking, Si—O and C—O bond formation, and the subsequent desorption of CO or CO₂ species from the surface. This mechanism leads to the room-temperature formation of a silicon oxide layer on the $\beta\text{-SiC}(100)$ surface which is basically free from carbon species. Subsequent annealing leads to the formation of a considerable amount of stoichiometric SiO₂ oxide leading to the formation of a Si oxide/ $\beta\text{-SiC}(100)$ interface in which silicon dioxide is dominant [Fig. 8(a)]. In fact, as in the cases of direct and promoted silicon oxidation, this interface is not abrupt, but includes substoichiometric oxide species, with silicon atoms bonded to one, two, and three oxygen atoms (Si⁺, Si²⁺, and Si³⁺), which are predominantly present at the internal interface and substrate surface.

We now turn to the discussion of the micromechanisms of Rb-promoted oxidation. By a simple comparison of the O 1s core-level intensity for both direct and promoted oxidation (Figs. 5, 6, and 7), it is obvious that the presence of the Rb monolayer on the $\beta\text{-SiC}(100)$ interface enhances dramatically the oxygen molecule sticking coefficient, even in the low-exposure regime. It leads to the very large enhancement of the oxygen uptake by four orders of magnitude. The high sticking probability is a common feature which has been observed on several alkali-covered semiconductor surfaces, such as Si.^{29,31,33} The alkali-metal-promoted dissociation of oxygen has also been demonstrated by valence-band studies on InP(110),⁵³ and can be explained by an efficient dissociation process mediated by charge transfer into the antibonding orbitals of the O₂ molecules.^{31,33,39} Apparently this mechanism takes place also for the present case of Rb-modified $\beta\text{-SiC}(100)$. Another important point which explains the enhanced sticking probability has been illustrated by a theoretical study, using *ab initio* molecular cluster calculations based on the local density functional theory for the prototypical K/Si(100) system, showing that the adsorption energy for oxygen molecules is in-

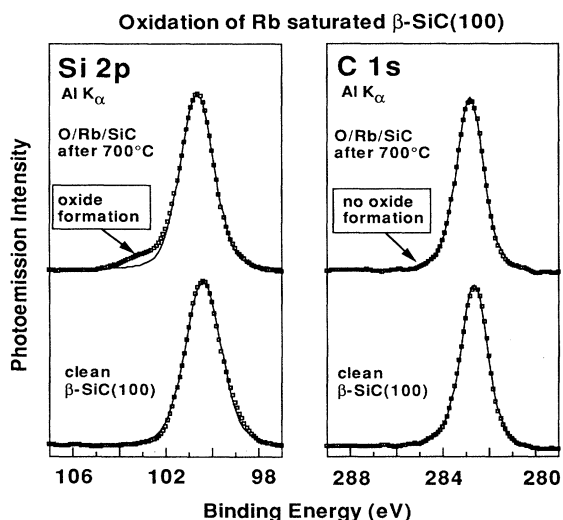


FIG. 11. Comparison of the oxide formation at Si 2*p* and C 1s core-level lines after Rb-promoted oxidation and thermal annealing at 700°C. The solid lines indicate single-peak fits to the data points. All spectra are taken in a bulk sensitive mode at a photon energy of 1486.6 eV. Squares represent the data points, and the single-peak fit is shown by the solid line.

creased by 0.24 eV in the presence of the alkali-metal overlayer.³⁹

Similar to other semiconductor substrates, the formation of alkali-metal oxides can be excluded,^{37,38} which is evidenced by looking at the O 1s core level which does not exhibit an alkali-oxide-related component: the O 1s peak *B*, which scales with the alkali-metal coverage, shows up already at the lowest oxygen exposures and/or low alkali-metal coverages, excluding the possibility of an interpretation in terms of a Rb-oxide related core-level shift. Furthermore, the O 1s peak *B* binding energy does not match to any of the known line positions of bulk alkali-metal oxides.³⁷ This situation is similar to the case of silicon surfaces where the same O 1s component *B* is related to O atoms weakly bonded only to the alkali-metal-substrate complex.³⁷ Another way to trace the possible formation of Rb oxides would be to look at the existence of a chemical shift at the Rb 3*p* core levels. Although such a feature could possibly be compensated by final states effects, the lack of a clear chemical shift at the Rb 3*p* core level [Fig. 8(b)] further supports the picture of no alkali-oxide formation. When the β -SiC(100) surface modified by a Rb monolayer is exposed to oxygen, the Rb 3*p* core level [Fig. 8(b)] is in fact just slightly affected with a 10% energy broadening only. This results from oxygen atoms chemisorbed to the Rb atoms through a weak bonding rather than from Rb oxide formation. In these views, it is interesting to notice that a totally different situation could be observed for alkali-metal-promoted oxidation of a metal surface such as aluminum modified by Na or K, with a clear evidence of alkali-oxide formation from large chemical shifts observed at Na 2*p* or K 3*p* alkali core levels,^{38,58} which are not observed here for SiC as in the case of semiconductor surfaces modified by alkali-metal atoms in the monolayer range coverage.³⁸

Another important step in the promotion mechanism is the enhanced migration rate of oxygen atoms underneath the surface breaking the substrate backbonds. This can be seen in Fig. 7 by comparing the uptake curves of the total integrated O 1s intensity for the bare SiC surface with the O 1s *A* component intensity for Rb-modified SiC. The latter component is related to oxygen-substrate bonding only and therefore indicates the amount of O atoms diffused into the bulk which contribute in the oxide formation. It can be seen that the uptake curves show a linear increase with the logarithm of the oxygen exposure (Fig. 7). The same behavior has also been observed in the oxide growth for the promoted oxidation of the Si(100)2 \times 1 surface by various alkali-metal atoms.³⁵ In these cases, it was demonstrated that the amount of silicon oxides formed on the surface and the oxygen uptake both strictly follow a linear law versus the logarithm of oxygen exposures and do not depend on the alkali-metal coverage.^{35,37} This behavior reflects the diffusion process of oxygen atoms underneath the surface into the bulk, which is the limiting factor for the oxide formation after room-temperature oxygen exposure. The much higher intensity of the O 1s *A* component for Rb/SiC(100) compared to the O 1s total intensity for bare SiC (Fig. 7) clearly indicates the effect of the alkali overlayer which facilitates the oxygen migration into the bulk and the

substrate backbond breaking. Detailed studies of the alkali-metal–Si system revealed that this effect is mediated by the covalent bonding nature of the metal adsorbate, which induces a weakening of the substrate backbonds.³¹ If this is also the case for the Rb-covered SiC surface, one cannot make any definitive conclusion on the ground of the present study. Our results show, however, that Rb chemisorption does not result in large SiC(100) surface disruption, as evidenced from the lack of large core-level shift at the Si 2*p* and C 1s core levels. Also, from the work-function measurements, one can deduce that the Rb/ β -SiC(100) surface/interface formation behavior appears to be very close to the one observed for elemental semiconductor systems such as alkali-metal–silicon surfaces. Therefore, the weakening of backbonds appears to be present also on the β -SiC(100) surface, which would certainly improve the surface reactivity and facilitate its interaction with the oxygen atoms. However, an investigation including high resolution core-level photoemission spectroscopy using synchrotron radiation would definitively be necessary to confirm this view.

Thermal annealing leads to an improved stoichiometry of the oxide layer, which is mediated by the thermally activated interdiffusion of oxygen and substrate atoms. As already outlined above, the carbon oxide species leave the surface by thermal desorption into the vacuum and a carbon-free silicon oxide layer dominantly composed of SiO₂ remains on the substrate after annealing at temperatures up to 440 °C [see Figs. 8(a) and 10]. The heating results also in the gradual removal of the Rb catalyst from the surface by thermal desorption, with no more Rb atoms present on the surface at 780 °C. One should notice that this Rb desorption temperature is significantly higher than observed for silicon surfaces, where temperatures between 550 to 650 °C are required.^{29–31,33} It suggests that Rb atoms are more tightly bound to the surface on β -SiC(100) than on Si(100)2 \times 1. Interestingly, *ab initio* DMOL molecular force calculations for the K/Si(100)2 \times 1 system have shown that, upon impinging oxygen molecules, the K–Si distance is relaxed by 5%, which gives rise to a bond weakening.³⁹ A similar behavior could also be expected here, which would explain the relative easy bond-breaking between the alkali-metal and the substrate atoms upon rising temperature, finally leading to an alkali-metal-free oxide layer on the β -SiC(100) surface. Such an interesting feature has already been successfully achieved for alkali-metal (Na, K, Rb, and Cs)-promoted oxidation of elemental semiconductor surfaces such as Si(100)2 \times 1 or Si(111)7 \times 7.^{29–31,33,59,60} However, this approach has been shown to fail for other compound semiconductors like III–V because of the low thermal stability of their oxides⁵⁴ and/or surface/interface disruption at rather low temperatures.⁶¹

V. CONCLUSIONS

We have investigated the direct and Rb-promoted oxidation of a β -SiC(100) surface by core-level photoemission spectroscopy. A clean and stoichiometric SiC surface could be obtained using sequences of careful anneal-

ings only. Direct room-temperature O₂ exposures of the clean β-SiC(100) surface result only in little oxygen uptake. In contrast, the presence of a Rb monolayer on the β-SiC(100) surface, which decreases the surface work function by -3.3 eV, is found to increase the room-temperature oxygen uptake by a factor of 10⁺⁴ leading into the formation of high silicon oxidation states. Carbon oxide species are not found on the surface, which can be addressed to the formation of CO and CO₂ molecules desorbing into the vacuum. Unlike other compound semiconductors such as III-V, this process leads to the selective formation of silicon oxides only on the β-SiC(100) surface. The micromechanisms of catalysis for this prototypical IV-IV compound semiconductor and the role of Rb appear to be close to the described steps for alkali-metal-promoted oxidation of elemental semi-

conductors such as silicon. Subsequent annealing at temperatures up to 700°C leads to the formation of a carbon-free silicon oxide layer with a strong reduction of the Rb overlayer, leading to the formation of a nonabrupt SiO₂/β-SiC(100) interface having lower oxidation states near the SiC(100) surface at lower temperatures than by direct thermal oxidation. The Rb atoms are completely removed from the surface at temperatures below 780°C.

ACKNOWLEDGMENTS

This work was supported by the European Union (EU) under Contract No. Science ERBSC1*CT915110. The authors are grateful to Ph. Brun for expert and outstanding technical assistance.

*Present address: Friedrich-Schiller-Universität Jena, Institut für Festkörperphysik, Jena, Germany.

†Also at DEA Science des Matériaux, Université Pierre et Marie Curie, 75252 Paris Cedex, France.

¹R. F. Davis, *J. Vac. Sci. Technol. A* **11**, 829 (1993).

²M. Dayan, *J. Vac. Sci. Technol. A* **4**, 38 (1985).

³Y. Mizokawa, K. M. Geib, and C. W. Wilmsen, *J. Vac. Sci. Technol. A* **4**, 1696 (1986).

⁴T. M. Parrill and V. M. Bermudez, *Solid State Commun.* **63**, 231 (1987).

⁵R. Kaplan, *Surf. Sci.* **215**, 111 (1989).

⁶S. Hara, W. F. J. Slijkerman, J. F. van der Veen, I. Ohdomari, S. Misawa, E. Sakuma, and S. Yoshida, *Surf. Sci. Lett.* **231**, L196 (1990).

⁷J. M. Powers, A. Wander, P. J. Rous, M. A. van Hove, and G. A. Somorjai, *Phys. Rev. B* **44**, 11 159 (1991).

⁸T. N. Parrill and Y. W. Chung, *Surf. Sci.* **243**, 96 (1991).

⁹V. M. Bermudez and R. Kaplan, *Phys. Rev. B* **44**, 11 149 (1991).

¹⁰J. M. Powers, A. Wander, M. A. van Hove, and G. A. Somorjai, *Surf. Sci. Lett.* **260**, L7 (1992).

¹¹E. Gat, B. Cros, R. Berjoan, and J. Durand, *Appl. Surf. Sci.* **64**, 345 (1993).

¹²M. Diani, J. L. Bischoff, L. Kubler, and D. Bolmont, *Appl. Surf. Sci.* **68**, 575 (1993).

¹³N. Becourt, B. Cros, J. L. Ponthenier, R. Berjoan, A. M. Papon, and C. Jaussaud, *Appl. Surf. Sci.* **68**, 461 (1993).

¹⁴P. Badziag, *Surf. Sci.* **236**, 48 (1990).

¹⁵Y. Mizokawa, S. Nakanishi, O. Komoda, S. Miyase, H. S. Diang, C. H. Wang, N. Li, and C. Jiang, *J. Appl. Phys.* **67**, 264 (1990).

¹⁶P. Badziag, *Phys. Rev. B* **44**, 11 143 (1991).

¹⁷B. I. Craig and P. V. Smith, *Surf. Sci.* **233**, 255 (1992).

¹⁸W. Zhu, X. H. Wang, B. R. Stoner, G. H. M. Ma, H. S. Kong, M. W. H. Braun, and J. T. Glass, *Phys. Rev. B* **47**, 6529 (1993).

¹⁹W. C. Lu, K. M. Zhang, and Xie Xide, *Phys. Rev. B* **48**, 18 159 (1993).

²⁰P. Käckell, B. Wenzien, and F. Bechstedt, *Phys. Rev. B* **50**, 10 761 (1994); B. Wenzien, P. Käckell, and F. Bechstedt, *Surf. Sci.* (to be published).

²¹L. Porte, *J. Appl. Phys.* **60**, 635 (1986).

²²D. W. Niles, H. Höchst, G. W. Zajac, T. H. Fleisch, B. C. Johnson, and J. M. Meese, *J. Vac. Sci. Technol. A* **6**, 1584 (1988); *J. Appl. Phys.* **65**, 662 (1989).

²³K. M. Geib, C. Wilson, R. G. Long, and C. W. Wilmsen, *J. Appl. Phys.* **68**, 2796 (1990).

²⁴T. N. Parrill and Y. W. Chung, *Surf. Sci.* **271**, 395 (1991).

²⁵V. M. Bermudez, *J. Appl. Phys.* **66**, 6084 (1989); *Surf. Sci.* **276**, 59 (1992).

²⁶J. M. Powers and G. A. Somorjai, *Surf. Sci.* **244**, 39 (1991).

²⁷W. A. Henle, M. G. Ramsey, F. P. Netzer, R. Cimino, W. Braun, and S. Witzel, *Phys. Rev. B* **42**, 11 073 (1990).

²⁸K. Okuno, T. Ito, M. Iwami, and A. Hiraki, *Solid State Commun.* **34**, 493 (1980); A. Cros, J. Derrien, and F. Salvan, *Surf. Sci.* **110**, 471 (1981); A. D. Katnani, P. Perfetti, T. X. Zhao, and G. Margaritondo, *Appl. Phys. Lett.* **40**, 619 (1982); I. Abbati, G. Rossi, L. Calliari, L. Braicovich, I. Lindau, and W. E. Spicer, *J. Vac. Sci. Technol.* **21**, 409 (1982); J. Derrien and F. Riengen, *Surf. Sci. Lett.* **124**, L235 (1983); A. Cros, *J. Phys. (Paris)* **44**, 707 (1983); F. U. Hillebrecht, M. Ronay, D. Rieger, and F. J. Himpsel, *Phys. Rev. B* **34**, 5377 (1986).

²⁹P. Soukiassian, T. M. Gentle, M. H. Bakshi, and Z. Hurych, *J. Appl. Phys.* **60**, 4339 (1986); P. Soukiassian, M. H. Bakshi, Z. D. Hurych, and T. M. Gentle, *Phys. Rev. B* **35**, 4176 (1987).

³⁰M. C. Asensio, E. G. Michel, E. M. Oellig, and R. Miranda, *Appl. Phys. Lett.* **51**, 1714 (1987).

³¹P. Soukiassian and H. I. Starnberg, *Physics and Chemistry of Alkali Metal Adsorption*, edited by H. P. Bonzel, A. M. Bradshaw, and G. Ertl, *Materials Science Monographs* (Elsevier, Amsterdam, 1989), Vol. 57, p. 449 and references therein.

³²C. A. Papageorgopoulos and M. Kamaratos, *Surf. Sci.* **221**, 263 (1989).

³³H. I. Starnberg, P. Soukiassian, and Z. Hurych, *Phys. Rev. B* **39**, 12 775 (1989).

³⁴J. A. Schaefer, F. Ladders, Th. Allinger, S. Nannarone, J. Anderson, and G. L. Lapeyre, *Surf. Sci.* **211-212**, 1075 (1989).

³⁵H. I. Starnberg, P. Soukiassian, M. H. Bakshi, and Z. Hurych, *Surf. Sci.* **224**, 13 (1989).

³⁶G. Boishin, M. Tikhov, and L. Surnev, *Surf. Sci.* **257**, 190 (1991).

³⁷M. Riehl-Chudoba, S. Nishigaki, Y. Huttel, F. Semond, Ph. Brun, and P. Soukiassian, *Appl. Surf. Sci.* **65-66**, 840 (1993).

- ³⁸Y. Huttel, E. Bourdié, P. Soukiassian, P. S. Mangat, and Z. Hurych, *Appl. Phys. Lett.* **62**, 2437 (1993); *J. Vac. Sci. Technol. A* **11**, 2186 (1993).
- ³⁹Ye Ling, A. J. Freeman, and B. Delley, *Surf. Sci. Lett.* **239**, L526 (1990).
- ⁴⁰K. M. Schirm, P. Soukiassian, P. S. Mangat, Z. Hurych, L. Soonckindt, and J. J. Bonnet, *J. Vac. Sci. Technol. B* **10**, 1867 (1992); *Appl. Surf. Sci.* **68**, 417 (1993).
- ⁴¹P. Soukiassian, T. Kendelewicz, and Z. D. Hurych, *Phys. Rev. B* **40**, 12 570 (1989).
- ⁴²K. M. Schirm, P. Soukiassian, Y. Borensztein, S. Nishigaki, G. S. Dong, K. Hricovini, and J. E. Bonnet, *Appl. Surf. Sci.* **68**, 433 (1993).
- ⁴³N. Becourt, J. L. Ponthenier, A. M. Papon, and C. Jaussaud, *Physica B* **185**, 79 (1993).
- ⁴⁴P. Soukiassian, J. A. Kubby, P. Mangat, Z. Hurych, and K. M. Schirm, *Phys. Rev. B* **46**, 13 471 (1992); L. Spiess, P. S. Mangat, S. P. Tang, K. M. Schirm, A. J. Freeman, and P. Soukiassian, *Surf. Sci. Lett.* **289**, L631 (1993).
- ⁴⁵P. Soukiassian, R. Riwan, Y. Borensztein, and J. Lecante, *J. Phys. C* **17**, 1761 (1984).
- ⁴⁶C. D. Wagner, L. E. Davis, M. V. Zeller, J. A. Taylor, R. H. Raymond, and L. H. Gale, *Surf. Interface Anal.* **3**, 211 (1981).
- ⁴⁷L. Muelhoff, W. J. Choyke, M. J. Bozack, and J. T. Yates, *J. Appl. Phys.* **60**, 2842 (1986).
- ⁴⁸P. Soukiassian, M. H. Bakshi, H. I. Starnberg, Z. Hurych, T. Gentle, and K. P. Schuette, *Phys. Rev. Lett.* **59**, 1488 (1987).
- ⁴⁹Y. Enta, T. Kinoshita, S. Suzuki, and S. Kono, *Phys. Rev. B* **36**, 9801 (1987).
- ⁵⁰T. E. Ortega, E. M. Oellig, J. Ferron, and R. Miranda, *Phys. Rev. B* **36**, 6213 (1987).
- ⁵¹P. Soukiassian, in *Fundamental Approach to New Materials Phases—Ordering at Surfaces and Interfaces*, edited by A. Yoshimori, T. Shinjo, and H. Watanabe, Springer Series in Materials Science Vol. 17 (Springer-Verlag, Berlin, 1992), p. 197 and references therein.
- ⁵²W. Braun and H. Kuhlenbeck, *Surf. Sci.* **180**, 279 (1986); M. Tabe, T. T. Chiang, I. Lindau, and W. E. Spicer, *Phys. Rev. B* **34**, 2706 (1986) and references therein.
- ⁵³P. Soukiassian, M. H. Bakshi, and Z. Hurych, *J. Appl. Phys.* **61**, 2679 (1987); P. Soukiassian, M. H. Bakshi, H. I. Starnberg, A. S. Bommanavar, and Z. Hurych, *Phys. Rev. B* **37**, 6496 (1988).
- ⁵⁴R. Miranda, M. Prietsch, C. Laubschat, M. Domke, T. Mandel, and G. Kaindl, *Phys. Rev. B* **39**, 10 387 (1989).
- ⁵⁵P. Sjövall, B. Hellsing, K. E. Keck, and B. Kasemo, *J. Vac. Sci. Technol. A* **5**, 1065 (1987).
- ⁵⁶B. Hellsing, *Phys. Rev. B* **40**, 3855 (1989).
- ⁵⁷M. Besançon, H. Araghi-Kozaz, R. Landers, and J. Jupille, *Surf. Sci.* **236**, 23 (1990).
- ⁵⁸N. A. Braaten, J. K. Grepstad, S. Raaen, and S. L. Qiu, *Surf. Sci.* **250**, 51 (1991).
- ⁵⁹P. Soukiassian, H. I. Starnberg, and T. Kendelewicz, *Appl. Surf. Sci.* **41-42**, 395 (1989).
- ⁶⁰H. I. Starnberg, P. Soukiassian, M. H. Bakshi, and Z. Hurych, *Phys. Rev. B* **37**, 1315 (1988).
- ⁶¹P. Soukiassian, T. Kendelewicz, H. I. Starnberg, M. H. Bakshi, and Z. Hurych, *Europhys. Lett.* **12**, 87 (1990); P. Soukiassian, P. S. Mangat, Y. Huttel, Z. Hurych, B. Gruzza, and A. Porte, *J. Vac. Sci. Technol. B* **11**, 1603 (1993).